Journal of Applied Mechanics and Technical Physics, Vol. 47, No. 1, pp. 12–21, 2006

FRICTION AND HEAT TRANSFER IN A LAMINAR SEPARATED FLOW BEHIND A RECTANGULAR STEP WITH POROUS INJECTION OR SUCTION

S. R. Batenko and V. I. Terekhov

UDC 532.517.2 + 532.526

Results of a numerical study of a laminar separated flow behind a rectangular step on a porous surface with uniform injection or suction are described. Two cases are considered: an unconfined flow past a step and flow evolution in a confined channel (duct). It is shown that mass transfer on the surface causes strong changes in the flow structure and substantially affects the position of the reattachment point, as well as friction and heat transfer. More intense injection leads first to an increase in the separation-zone length and then to its rapid vanishing due to boundary-layer displacement. Vice versa, suction at high Reynolds numbers $\mathrm{Re}_s > 100$ *reduces the separation-zone length. The duct flow has a complicated distribution of friction and heat-transfer coefficients along the porous surface owing to the coupled effect of the transverse flow of the substance and changes in the main flow velocity due to mass transfer.*

Key words: *flow separation and reattachment, laminar flow, porous injection and suction, backward-facing step, friction, heat transfer.*

Introduction. Injection or suction of a gas through a porous wall is an effective method of controlling flow parameters and heat transfer both in laminar and turbulent boundary layers. Porous injection can be used to completely displace the boundary layer away from the wall, whereas friction and heat transfer on the surface vanish. Porous suction, vice versa, enhances heat and mass transfer, and the transfer processes can be substantially intensified in the asymptotic suction mode.

The influence of permeability of the wall on characteristics of attached boundary layers has been studied in many experimental and theoretical works, which were reviewed in the monographs [1, 2]. At the same time, there are only few publications on flow separation and reattachment on a permeable surface [3–8], despite of problem importance. Among those papers, both experimental and theoretical activities deal with a turbulent flow regime and with porous injection only; the effect of suction on parameters of the separated flow and heat transfer have not been considered.

All above-mentioned papers revealed a strong effect of porous injection on the separation-zone length, shape of velocity profiles, and, correspondingly, distributions of friction and heat-transfer coefficients. The results of the researches performed, however, are contradictory. Thus, a higher injection velocity was argued to shift the reattachment point farther from the separation point [4, 5] and to reduce the separation-zone length [7]. According to the experiments of [7], the coordinate of the flow-reattachment point is severely affected by the free-stream temperature. There is no qualitative agreement in heat-transfer measurements either. Thus, Shishov et al. [3] found that injection reduces heat-transfer intensity, as it occurs in the attached flow, whereas the results of Ying-Tang and Chun-Hung [7] suggest that heat transfer becomes more intense with increasing velocity of gas injection through a porous wall. These contradictions can be attributed to numerous reasons, and the primary reason can be

Kutateladze Institute of Thermophysics, Siberian Division, Russian Academy of Sciences, Novosibirsk 630090; terekhov@itp.nsc.ru. Translated from Prikladnaya Mekhanika i Tekhnicheskaya Fizika, Vol. 47, No. 1, pp. 18–28, January–February, 2006. Original article submitted August 4, 2004; revision submitted January 31, 2005.

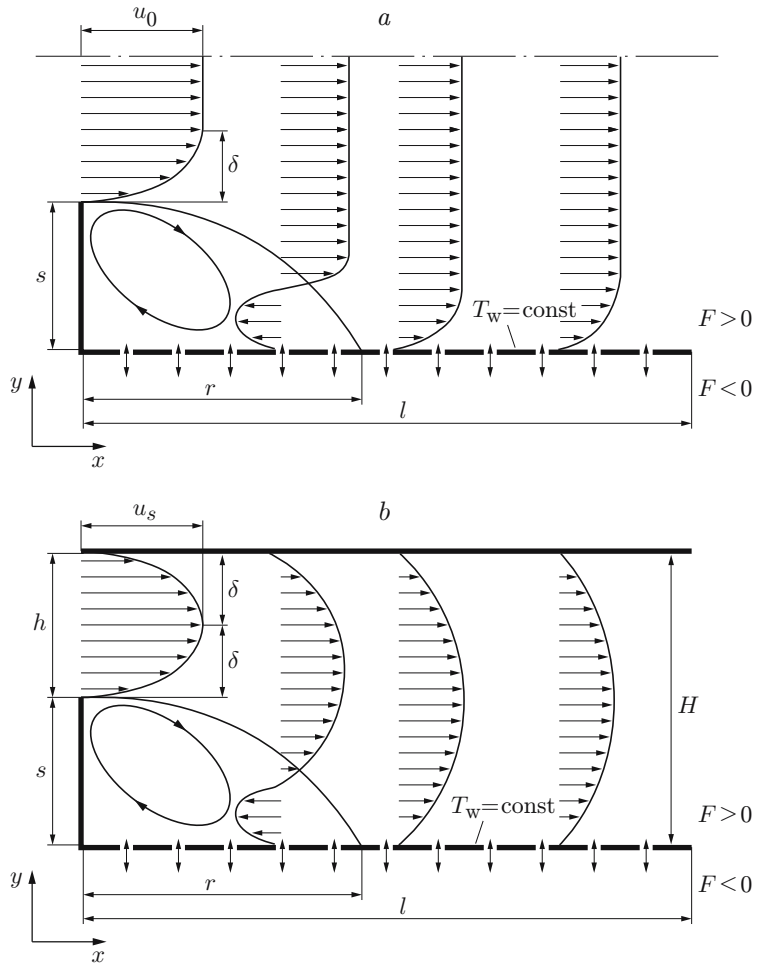

Fig. 1. Schematic of a separated flow behind a backward-facing step with a permeable surface: separation of an unconfined flow (a) and duct flow (b).

assumed to be the effect of mass addition on the main flow. In the case of intense injection in ducts of limited size, this effect can be fairly significant; therefore, a change in the duct geometry can cardinally alter aerodynamics and heat and mass transfer. This is evidenced by results for simpler conditions [9, 10], where there is no mass transfer on the surface, and changes in the duct expansion ratio (ER) lead to cardinal reconstruction of the flow and mass transfer (ER = H/h, where h and H are the duct heights before and after flow separation).

As was shown in [9–13], separation of a laminar flow behind a step without mass transfer has not been adequately studied, and intense research is going on. A pioneering study of the influence of permeability of the wall on separation and reattachment of a laminar flow was described in [14]. The objective of the present paper, which continues the research started in [14], is a numerical analysis of the influence of porous injection and suction on aerodynamics and heat transfer in the case of separation of a laminar flow behind a backward-facing rectangular step. The calculations were performed for an unconfined flow past a step and for a duct flow.

Formulation of the Problem. Governing Equations and Solution Technique. The flow past a step is schematically shown in Fig. 1. In the first case (Fig. 1a), a rectangular step of height s is exposed to an unconfined incompressible fluid flow with constant physical properties and with a velocity u_0 in the undisturbed flow core. The thickness of the boundary layer ahead of its separation from the step is $\delta = s/2$, and the velocity profile follows the parabolic distribution

$$u/u_0 = 2\zeta - \zeta^2, \tag{1}$$

where $\zeta = y/\delta$; the coordinate y is counted from the upper edge of the step.

In the second case (Fig. 1b), flow separation occurs in a duct of limited size. The duct height before and after expansion is s and $2s$, respectively (s is the step height). The duct-expansion parameter in this case is ER = 2. To simplify the calculations, we assumed that the velocity profile ahead of the separation point corresponded to a developed laminar flow, and the boundary-layer thickness $h = s/2$ was identical to that in the unconfined flow.

The duct length behind the step in both cases was $l/s = 50$, and the vertical size of the computational domain for the unconfined flow was $H/s = 30$. The lower wall of the duct was permeable: it was used for injection (suction) of a gas whose composition was identical to that of the main flow (air) with a constant velocity v_{w} over the duct length. The injection (suction) parameter was determined by the ratio $F = v_{\mathrm{w}}/u_0$, where u_0 was the velocity in the flow core in the case of the unconfined flow or the mean-mass velocity in the cross section of the step in the case of the duct flow. Positive and negative values of F corresponded to gas injection and suction, respectively.

The temperature of the porous wall was assumed to be unchanged along the duct ($T_{\mathrm{w}} = \mathrm{const}$), and the remaining surfaces were adiabatic; there was no initial heat layer ahead of flow separation.

The flow was calculated for Reynolds numbers $\mathrm{Re}_s = u_0 s/\nu = 10$–$1000$ (ν is the kinematic viscosity), the permeability parameter being varied within a wide range: $10^{-4} \leqslant |F| \leqslant 10^{-1}$. The problem calculation was based on solving a two-dimensional system of elliptic Navier–Stokes equations and a heat-transfer equation:

$$\begin{gathered}
\frac{\partial u}{\partial t} + u\,\frac{\partial u}{\partial x} + v\,\frac{\partial u}{\partial y} = -\frac{1}{p}\,\frac{\partial p}{\partial x} + \nu\Big[\frac{\partial^2 u}{\partial x^2} + \frac{\partial^2 u}{\partial y^2}\Big], \\
\frac{\partial v}{\partial t} + u\,\frac{\partial v}{\partial x} + v\,\frac{\partial v}{\partial y} = -\frac{1}{p}\,\frac{\partial p}{\partial y} + \nu\Big[\frac{\partial^2 v}{\partial x^2} + \frac{\partial^2 v}{\partial y^2}\Big], \\
\frac{\partial u}{\partial x} + \frac{\partial v}{\partial y} = 0, \\
\frac{\partial T}{\partial t} + u\,\frac{\partial T}{\partial x} + v\,\frac{\partial T}{\partial y} = \frac{1}{\mathrm{Pe}}\Big[\frac{\partial^2 T}{\partial x^2} + \frac{\partial^2 T}{\partial y^2}\Big].
\end{gathered} \tag{2}$$

Here t is the time, T is the temperature, p is the pressure, and Pe is the Peclet number.

To simplify the calculations, we divided the problem into two stages. First, numerical simulations of aerodynamics were performed by solving unsteady Navier–Stokes equations written for a fluid with constant physical properties in the stream function–vorticity variables by an iterative procedure:

$$\begin{gathered}
\frac{\partial \xi}{\partial \tau} + \frac{\partial u\xi}{\partial x} + \frac{\partial v\xi}{\partial y} = \frac{1}{\mathrm{Re}_s}\Big(\frac{\partial^2 \xi}{\partial x^2} + \frac{\partial^2 \xi}{\partial y^2}\Big), \\
\frac{\partial^2 \psi}{\partial^2 x} + \frac{\partial^2 \psi}{\partial y^2} = \xi, \\
u = \frac{\partial \psi}{\partial y}, \qquad v = -\frac{\partial \psi}{\partial x}.
\end{gathered} \tag{3}$$

Based on the velocity field obtained by solving the heat-transfer equation

$$\frac{\partial^2 \theta}{\partial \tau} + \frac{\partial u\theta}{\partial x} + \frac{\partial v\theta}{\partial y} = \frac{1}{\mathrm{Pe}}\Big(\frac{\partial^2 \theta}{\partial x^2} + \frac{\partial^2 \theta}{\partial y^2}\Big), \tag{4}$$

we found the steady-state distribution of temperature. Here $\theta = (T - T_0)/(T_{\mathrm{w}} - T_0)$, where T_0 is the gas temperature at the duct entrance or in the free stream. Equations (3) and (4) are written in dimensionless form. The characteristic values of variables for normalization were the step height s, velocity u_0, and time interval s/u_0.

The steady-state solutions of Eqs. (3), (4) were found by iterations with asymptotic stabilization in time. An implicit scheme of the alternating direction method was used [15]. Upwind differences with the first-order accuracy for steps of spatial variables were used for discretization of convective terms, and second-order central differences were used for diffusion terms.

To solve the dynamic equations, the no-slip condition $u = v = 0$ was imposed on impermeable walls, which corresponded to the relation $\psi = \mathrm{const}$ and Woods' condition in the stream function–vorticity variables:

$$\xi_{\mathrm{w}} + \frac{1}{2}\,\xi_{\mathrm{w}+1} + 3\,\frac{\psi_{\mathrm{w}} - \psi_{\mathrm{w}+1}}{\Delta x^2} + O(\Delta x^2) = 0,$$

$$\xi_{\rm w} + \frac{1}{2}\,\xi_{\rm w+1} + 3\,\frac{\psi_{\rm w} - \psi_{\rm w+1}}{\Delta y^2} + O(\Delta y^2) = 0.$$

To solve the heat-transfer equation, the adiabaticity condition ($\partial\theta/\partial x = 0$ and $\partial\theta/\partial y = 0$) was set on impermeable walls. In the case of injection (suction) through the lower wall, the boundary condition on the stream function was $\psi(x) = -Fx$, and Woods' condition was also used for vorticity. The output boundary was subjected to soft boundary conditions for the stream function, vorticity, and temperature:

$$\frac{\partial^2\psi}{\partial x^2} = 0, \qquad \frac{\partial^2\xi}{\partial x^2} = 0, \qquad \frac{\partial^2\theta}{\partial x^2} = 0. \tag{5}$$

In the unconfined flow past the backward-facing step, the boundary conditions for the stream function and vorticity at the upper boundary were formulated in the following form:

$$\frac{\partial\psi}{\partial y} = 1, \qquad \frac{\partial\xi}{\partial y} = 0. \tag{6}$$

The friction C_f and heat-transfer α coefficients on the permeable wall were determined as

$$\frac{C_f}{2} = \frac{\tau_{\rm w}}{\rho u_0^2} = \frac{1}{{\rm Re}_s}\,\frac{\partial u}{\partial y}\Big|_{\rm w}; \tag{7}$$

$$\alpha = -\frac{\lambda}{s}\,\frac{\partial\theta}{\partial y}\Big|_{\rm w}, \qquad {\rm Nu}_s = \frac{\alpha s}{\lambda} = -\frac{\partial\theta}{\partial y}\Big|_{\rm w}, \tag{8}$$

where $\tau_{\rm w}$ is the friction stress on the wall, λ is the thermal conductivity, and ${\rm Nu}_s$ is the Nusselt number. The model was tested by comparing the numerical data with the experimental results of [16] in terms of the coordinate of the reattachment point for the flow in an unconfined duct without mass transfer on the surface. The calculation results are in good agreement with the experiment for ${\rm Re}_s \lesssim 600$. A further increase in the Reynolds number leads to a mismatch between the numerical and experimental data, which indicates that the flow transforms to a turbulent regime. Moreover, the calculation results were compared with a numerical analysis of the laminar flow past a step with different dynamic histories [9] though in the absence of injection (suction). The results of this part of comparisons also provided good agreement and allowed us to choose the optimal computational grid.

Grids with 100×300 nodes and 200×100 nodes were used in the unconfined flow and in the duct flow, respectively. Doubling or halving the number of nodes induced only minor changes in friction and heat-transfer coefficients (less than 1.2%). Uniform grids were used for both types of the flow examined.

Test Results and Discussion. The streamlines for the duct flow are plotted in Fig. 2. If there is no transverse flux of the substance, a typical recirculation (backflow) zone with a clearly expressed point of flow reattachment to the wall is formed on the wall behind the step (Fig. 2a). As was shown in experiments and calculations [10, 16], the influence of separation extends up to the upper wall with formation of a local circulation zone. The dashed curves in Fig. 2a show the dividing streamlines.

In the case of intense injection (Fig. 2b), the recirculation zone behind the step is not formed. Immediately behind the step, however, the coupled action of separation and injection leads to formation of a region of negative shear stresses, which is then transformed into a region of positive stresses. Therefore, the point with zero shear stress cannot be considered as the point of reattachment of the separated flow, as this occurs in the case of separation without injection.

The separated flow structure in the case of porous suction is even more complicated (Fig. 2c). The recirculation region becomes shorter, and the flow-separation region on the upper wall becomes commensurable with the main separation bubble. The streamlines between these vortices are strongly curved.

Thus, injection and suction exert a strong effect on formation of the flow after its shedding from the step edge. Correspondingly, the magnitude of the transverse flow on the surface and its direction affect the basic parameters of the flow, such as the coordinate of the reattachment point, friction, and heat transfer. This postulate is validated by the data in Fig. 3, which shows the influence of injection (suction) on the position of the reattachment point in the unconfined flow (Fig. 3a) and in the duct flow (Fig. 3b). The position of the reattachment point was assumed to be the coordinate where the shear stress on the wall acquired the zero value ($\tau_{\rm w} = 0$).

For low Reynolds numbers (${\rm Re}_s < 200$), the transverse flow on the wall exerts practically no effect on the distance between the step and the reattachment point. Only in the case of intense injection ($F > 10^{-2}$), with

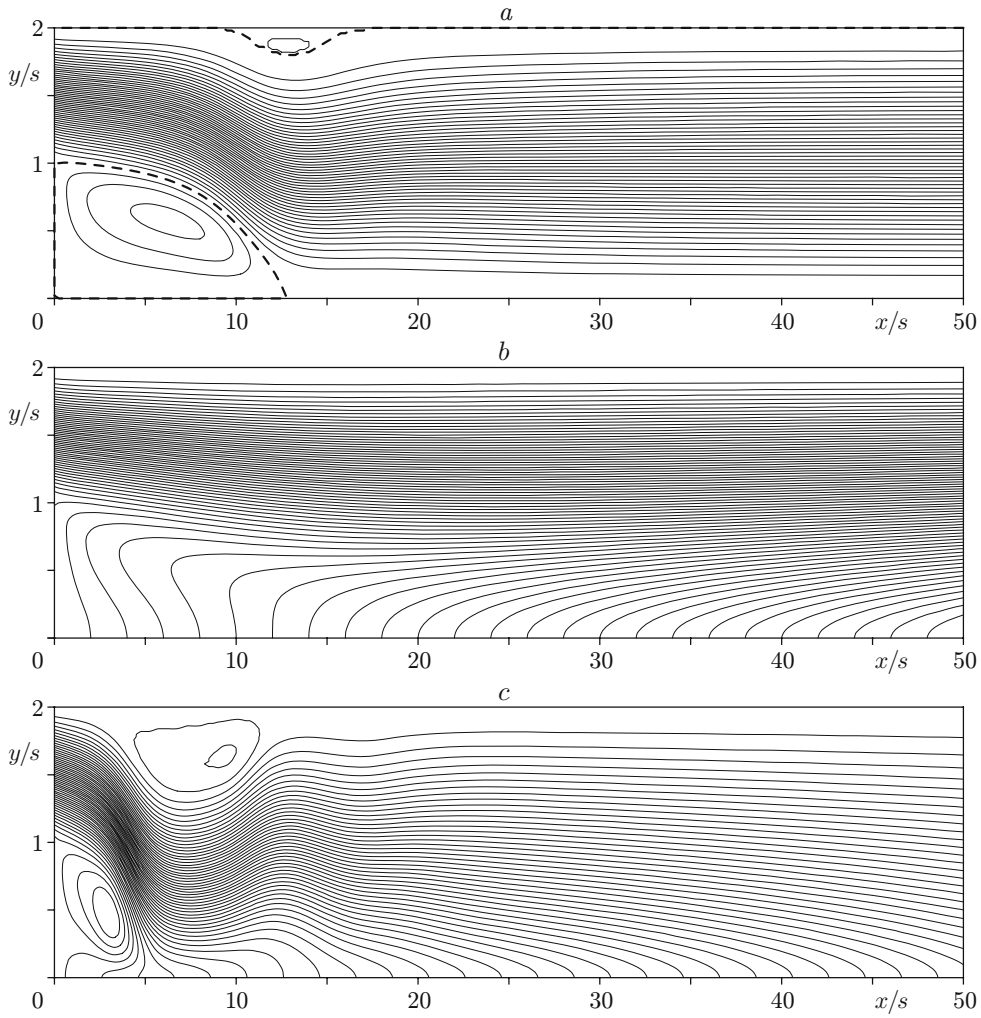

Fig. 2. Streamlines of flow separation in a duct (ER = 2 and $\mathrm{Re}_s = 400$) with an impermeable wall ($F = 0$) (a), with a permeable wall and porous injection ($F = 0.01$) (b), and with a permeable wall and porous suction ($F = -0.01$) (c).

displacement of the boundary layer away from the wall, the separation-region length vanishes. The circulation zone does exist, as was demonstrated by an analysis of the flow structure, but it becomes closed on the side surface of the step owing to its displacement from the surface of the lower wall.

For high Reynolds numbers ($\mathrm{Re}_s > 200$), the separation-region length increases with increasing dimensionless injection velocity ($F > 10^{-3}$). This is attributed to gradual displacement of the separation bubble, its shift in the downstream direction, and subsequent disintegration with complete separation of the flow from the wall. The point with zero friction is rapidly shifted toward the step base, and $r/s \to 0$.

A decrease in suction intensity at high Reynolds numbers leads to a smooth decrease in the vortex-zone length almost by a factor of 2 as compared with the impermeable surface.

A similar dependence of the reattachment-point coordinate on injection (suction) is observed in the case of flow separation in the duct (Fig. 3b). The only difference from the unconfined flow is that the reattachment point is shifted much farther downstream in the duct, especially at high Reynolds numbers, and the flow displacement from the wall occurs almost at identical injection intensities.

The calculated skin-friction coefficient along the porous plate with a varied injection (suction) parameter are shown in Fig. 4. As it could be expected, injection into an unconfined flow past a step (Fig. 4a) reduces friction both in the recirculation region and behind the reattachment point. In the case of intense injection ($F > 10^{-2}$),

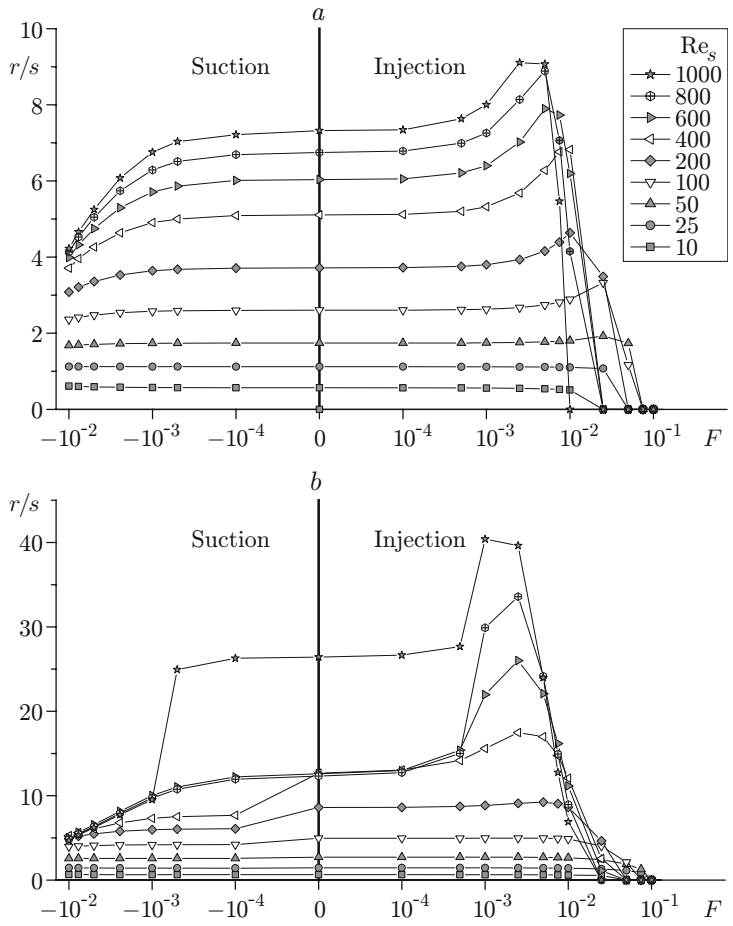

Fig. 3. Separation-region length in the presence of mass transfer on the surface: unconfined flow past a step (a) and duct flow (ER = 2) (b).

friction on the plate is close to zero everywhere, which testifies to boundary-layer displacement. Suction, vice versa, increases friction both in the separation region and behind flow reattachment. In the case of intense suction, the friction coefficient behind flow reattachment depends no longer on the streamwise coordinate, which indicates the transition to the asymptotic suction mode.

In the case of flow separation in the duct (Fig. 4b), the streamwise distribution of the friction coefficient has a more complicated character. Additional minimums and maximums in the friction-coefficient curve appear, which are not observed in the case of an unconfined flow. The reason for this behavior of C_f is the fact that the magnitude of friction for a duct flow is affected, in addition to the transverse flow of the substance, by changes in the mean streamwise velocity due to gas-mass addition or removal through the wall. The mean velocity in the duct increases in the streamwise direction in the case of injection and decreases in the case of suction. A decrease in friction in the case of porous injection and its increase in the case of suction finally lead to a dual effect of mass transfer on the wall and the change in the gas flow rate in the duct on the magnitude of skin friction. For this reason, apparently, all the calculation curves in Fig. 4b have a tendency to bunching toward the end of the duct. Obviously, the friction-coefficient distribution will be different in a different duct geometry. This distribution is also changed by Reynolds number variations, which is evidenced by the data plotted in Fig. 4c and obtained for $\mathrm{Re}_s = 1000$. It follows from Fig. 4c that a change in the permeability parameter leads to a significant scatter in the values of the friction coefficient in the flow-relaxation region.

Permeability of the surface has a significant effect on the thermal characteristics of the separated flow. This is illustrated in Fig. 5, which shows the streamwise distribution of the Nusselt number for different dimensionless injection (suction) velocities. As in an unconfined flow past a step (Fig. 5a), the heat-transfer intensity decreases

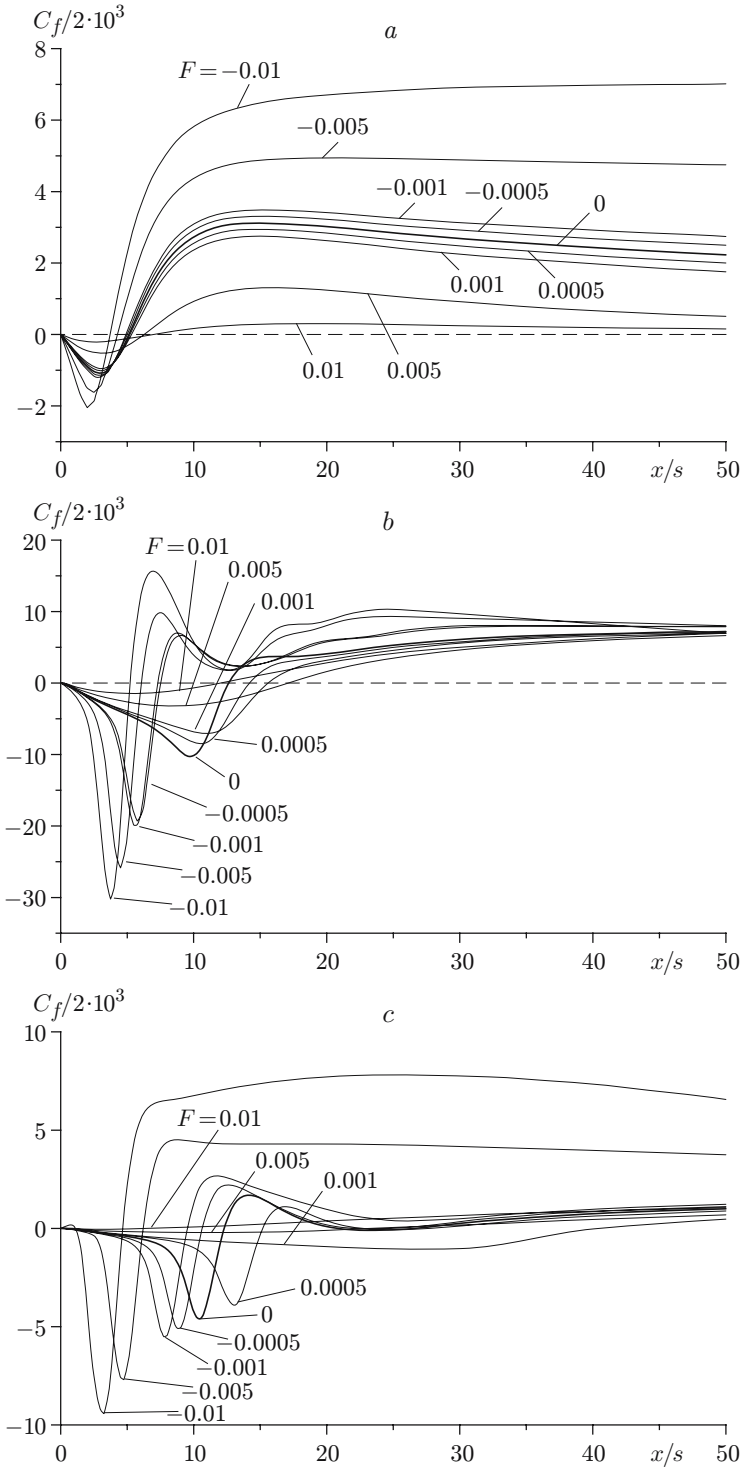

Fig. 4. Distribution of the friction coefficient along a permeable surface: (a) unconfined flow ($\mathrm{Re}_s = 400$); (b) duct flow (ER = 2 and $\mathrm{Re}_s = 400$); (c) duct flow (ER = 2 and $\mathrm{Re}_s = 1000$).

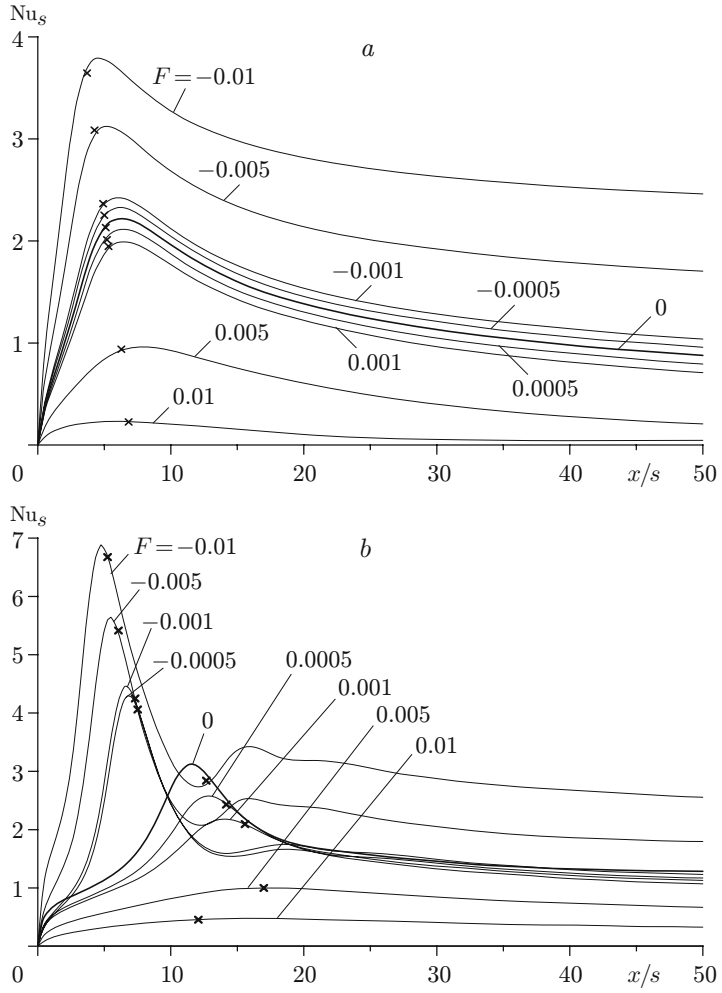

Fig. 5. Heat-transfer coefficient in a separated flow with a varied injection (suction) velocity ($\mathrm{Re}_s = 400$) for unconfined flow (a) and duct flow (ER = 2) (b); the points of flow reattachment ($C_f = 0$) are marked by crosses.

with increasing injection and increases with increasing suction, as it could be expected. In the case of boundary-layer suction, the maximums of heat transfer in the zone of flow reattachment are more clearly expressed and are shifted downstream from the reattachment point where $C_f/2 = 0$.

A more complicated distribution of the heat-transfer coefficient is observed in the case of flow separation in a duct (Fig. 5b). The reasons for this behavior were discussed above in analyzing the behavior of friction (see Fig. 4b). The point of flow reattachment does not coincide with the maximum of heat transfer, but the coordinate $\mathrm{Nu}_{s,\max}$ is shifted upstream, in contrast to an unconfined flow.

The maximum heat-transfer coefficient as a function of the injection (suction) parameter F is plotted in Fig. 6. The influence of mass transfer on the wall, as it follows from Fig. 6a, affects heat transfer for $|F| > 10^{-3}$. Boundary-layer displacement from the wall occurs in the region of intense injection ($F > 10^{-2}$); hence, $\mathrm{Nu}_s \to 0$. In the case of suction, heat transfer gradually increases, beginning from the values $|F| \approx 10^{-2}$, and this increase is more intense for high Reynolds numbers.

For the duct flow (Fig. 6b), the dependence of the maximum Nusselt number $\mathrm{Nu}_{s,\max}$ is approximately the same as that for unconfined flow separation. The absolute values of $\mathrm{Nu}_{s,\max}$ for the duct flow are higher than those for unconfined flow separation.

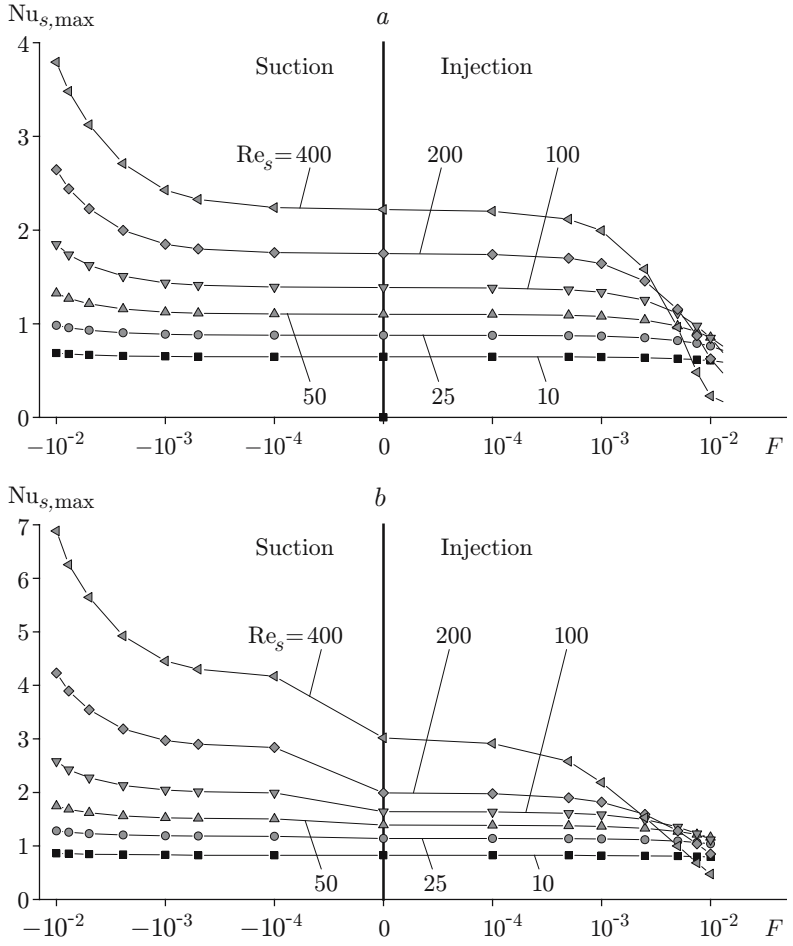

Fig. 6. Effect of injection (suction) intensity on the maximum heat-transfer coefficient for unconfined flow (a) and duct flow (ER = 2) (b).

Thus, injection and suction exert a strong effect on the flow structure, friction, and heat transfer in a separated laminar flow behind a rectangular step. The influence of these factors has a complicated and nonmonotonic character and is more pronounced in the case of flow separation in a duct, which is caused by flow confinement.

The authors are grateful to A. P. Grechanova for her assistance in numerical calculations.

This work was supported by the Russian Foundation for Basic Research (Grant No. 04-02-16070) and by the Foundation "Leading Scientific Schools of Russia" (Grant No. NSh-1308.2003.8).

REFERENCES

1. S. S. Kutateladze and A. I. Leont'ev, *Heat and Mass Transfer, and Friction in a Turbulent Boundary Layer* [in Russian], Énergiya, Moscow (1972).
2. V. M. Eroshenko and L. I. Zaichik, *Hydrodynamics and Heat and Mass Transfer on Permeable Surfaces* [in Russian], Nauka, Moscow (1984).
3. E. V. Shishov, P. S. Roganov, V. P. Zabolotskii, and R. Sh. Atayan, "Distributions of skin-friction coefficients and Stanton numbers behind a backward-facing step under porous injection," *Inzh.-Fiz. Zh.*, **53**, No. 4, 666–667 (1987).
4. J.-T. Yang, B. B. Tsai, and G. L. Tsai, "Separated-reattaching flow over a back step with uniform normal mass bleed," *Trans. ASME, J. Fluid Eng.*, **116**, 29–35 (1994).

5. Y. Yue-Tzu and K. Chung-Lun, "Numerical study of a backward-facing step with uniform normal mass bleed," *Int. J. Heat Mass Transfer*, **40**, No. 7, 1677–1686 (1997).
6. J.-T. Yang, J.-D. Gu, and W.-J. Ma, "Transient cooling effect by wall mass injection after backstep in high temperature flow field," *Int. J. Heat Mass Transfer*, **44**, 843–855 (2001).
7. Y. Ying-Tang and T. Chun-Hung, "High temperature heat transfer of separated flow over a sudden-expansion with base mass injection," *Int. J. Heat Mass Transfer*, **39**, 2293–2301 (1996).
8. B. A. A. Abu-Hijleh, "Heat transfer from a 2D backward facing step with isotropic porous floor segments," *Int. J. Heat Mass Transfer*, **43**, 2727–2737 (2000).
9. S. P. Batenko and V. I. Terekhov, "Effect of dynamic prehistory on aerodynamics of a laminar separated flow in a channel behind a rectangular backward-facing step," *J. Appl. Mech. Tech. Phys.*, **43**, No. 6, 854–860 (2002).
10. T. Kondoh, Y. Nagano, and T. Tsuji, "Computational study of laminar heat transfer downstream of a backward-facing step," *Int. J. Heat Mass Transfer*, **36**, 577–591 (1993).
11. W. Aung, A. Baron, and F.-K. Tsou, "Wall independency and effect of initial shear-layer thickness in separated flow and heat transfer," *Int. J. Heat Mass Transfer*, **28**, 1757–1771 (1985).
12. W. Aung, "An experimental study of laminar heat transfer downstream of a backstep," *J. Heat Transfer*, **105**, 823–829 (1983).
13. H. Iwai, K. Nakabe, K. Suzuki, and K. Matsubara, "Flow and heat transfer characteristics of backward-facing step laminar flow in a rectangular duct," *Int. J. Heat Mass Transfer*, **43**, 457–471 (2000).
14. S. R. Batenko, A. P. Grechanova, and V. I. Terekhov, "The effect of porous blowing and suction on aerodynamics and heat transfer in separated laminar flow in duct behind of backward-facing step," in: *Proc. of the XI Int. Conf. on the Methods of Aerophysical Research* (ICMAR), Novosibirsk, July 1–7, 2002, Part 1, Publ. House "Nonparel," Novosibirsk (2002), pp. 34–39.
15. P. J. Roache, *Computational Fluid Mechanics*, Hermosa, Albuquerque (1976).
16. B. F. Armaly, F. Durst, and J. C. F. Pereira, "Experimental and theoretical investigation of backward-facing step flow," *J. Fluid Mech.*, **127**, 473–496 (1983).